

Mapping the Physical and Chemical Conditions of the Ring Nebula

Marcelo L. Leal-Ferreira¹, Isabel Aleman^{1,2}, Andrea Gaughan³,
Djazia Ladjal^{4,5}, Toshiya Ueta⁶, Samuel Kerber⁶, Blair Conn^{4,5},
Rhiannon Gardiner⁶ and Alexander G. G. M. Tielens¹

¹Leiden Observatory, University of Leiden, PO Box 9513, 2300 RA, Leiden, The Netherlands

²IAG-USP, Universidade de São Paulo, Brazil, ³Haverford College, USA, ⁴Gemini Observatory, Chile, ⁵ANU, Australia ⁶University of Denver, USA, ⁷Monash University, Australia

Abstract. We observed the Planetary Nebula NGC 6720 with the Gemini Telescope and the Gemini Multi-Object Spectrographs. We obtained spatial maps of 36 emission-lines in the wavelength range between 3600 Å and 9400 Å. We derived maps of $c(\text{H}\beta)$, electronic densities, electronic temperatures, ionic and elemental abundances, and Ionization Correction Factors (ICFs) in the source and investigated the mass-loss history of the progenitor. The elemental abundance results indicate the need for ICFs based on three-dimensional photoionization models.

1. Introduction

Low- and intermediate-mass stars ($0.8\text{--}8 M_{\odot}$) turn into Planetary Nebulae (PNe) when the material ejected by the Asymptotic Giant Branch (AGB) progenitor star gets ionized by the remaining exposed core (central star). By investigating different spatial regions of the nebula, as in this work, we are able to access the mass-loss history of the source.

We performed slit scan observations of the PN NGC 6720 (Ring Nebula) with the 8.1 m Gemini telescope and the Gemini Multi-Object Spectrograph (GMOS). We extracted 36 emission-line maps from the data cube, as listed in Table 1. The table also shows the respective total flux of the maps, scaled to the total flux of $\text{H}\beta=100$.

We used the IDL tool 2D_Neb (Leal-Ferreira *et al.* 2011) to derive the maps of the extinction coefficient $c(\text{H}\beta)$, electronic densities (N_e) and temperatures (T_e), ionic and elemental abundances, and Ionization Correction Factors (ICFs) in the Ring Nebula. The 2D_Neb follows the formalism of the well-established iraf.nebular package (De Robertis *et al.* 1987; Shaw & Dufour 1995), and it is adapted to deal with two-dimensional spatial data. It was successfully used before in the analysis of the PNe NGC 40 (Leal-Ferreira *et al.* 2011), NGC 3243 (Monteiro *et al.* 2013), and Tc 1 (Aleman *et al.* in prep).

2. Results

In the last 2 columns of Table 1, we present the median of the $c(\text{H}\beta)$, N_e , T_e , and ionic abundance maps. Below we briefly discuss the $c(\text{H}\beta)$ map, while the remaining maps will be presented in a forthcoming paper. We also derived elemental abundances adopting the ICF method to correct for unobserved species. We used the ICFs from Kingsburgh & Barlow (1994) and concluded that the ICFs derived from one-dimensional photoionization models are insufficient to provide a reliable total abundance result when analyzing spatially-resolved data as in the present work.

The $c(\text{H}\beta)$ map was derived from the comparison of the observed to theoretical ratios of $\text{H}\alpha$, $\text{H}\gamma$, and $\text{H}\delta$ in respect to $\text{H}\beta$. Figure 1 shows the $c(\text{H}\beta)$ map (left), its histogram

Table 1. Emission-lines maps of the Ring Nebula extracted from the data cube.

Specie	Wavelength (Å)	Total Flux (Hβ= 100)	Specie	Wavelength (Å)	Total Flux (Hβ= 100)	Derived Property	Median Result
[O II]	3727	570.07	[O III]	5007	1013.73	c(Hβ)	0.26
H11	3771	0.02	[N I]	5199	2.09	N _e [S II] (cm ⁻³)	410
H10	3798	0.40	He I	5413	0.31	T _e [N II] (K)	7030
Hη	3836	0.63	[Cl III]	5517	0.04	T _e [O III] (K)	10690
[Ne III]	3869	138.38	[Cl III]	5537	7.e-3	He ⁺ /H ⁺	9.6E-2
Hζ	3890	19.20	[N II]	5755	2.06	He ⁺⁺ /H ⁺	1.9E-2
[Ne III]	3969	56.45	He I	5876	4.87	N ⁰ /H ⁺	1.2E-5
Hδ	4101	25.03	[O I]	6300	28.16	N ⁺⁺ /H ⁺	3.1E-4
C II	4268	7.e-3	[S III]	6312	0.39	O ⁰ /H ⁺	3.9E-4
Hγ	4341	45.15	[O I]	6363	9.66	O ⁺ /H ⁺	1.8E-3
[O III]	4363	7.23	[N II]	6548	144.87	O ⁺⁺ /H ⁺	2.4E-4
He I	4471	3.55	Hα	6563	296.94	Ne ⁺⁺ /H ⁺	1.3E-4
He I	4542	0.02	[N II]	6584	463.12	S ⁺ /H ⁺	4.7E-6
He I	4686	20.86	He I	6678	3.17	S ⁺⁺ /H ⁺	2.9E-6
[Ar IV]	4741	0.77	[S II]	6717	29.63	Cl ⁺⁺ /H ⁺	4.0E-8
Hβ	4861	100.00	[S II]	6737	28.72	Ar ⁺⁺ /H ⁺	2.9E-6
He I	4921	0.27	He I	7065	4.52	Ar ³⁺ /H ⁺	5.6E-7
[O III]	4959	345.20	[Ar III]	7136	39.40		

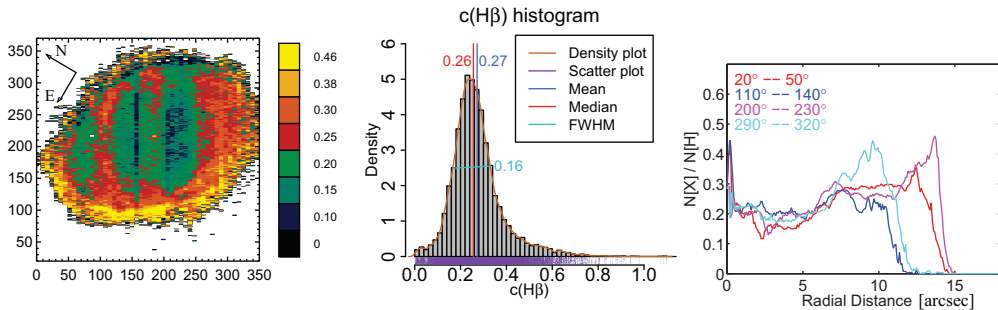


Figure 1. Extinction coefficient of NGC 6720 derived from Gemini/GMOS data. Left: Spatial distribution of $c(H\beta)$. Center: Its histogram (the median is shown in red, mean in blue, FWHM in cyan, density plot in dark orange, and scatter plot in purple). Right: Averaged radial profiles of $c(H\beta)$. The angles (indicated in the figure) increase counter-clockwise and 0° is to the right.

(center), and its averaged radial profile along 4 different directions (right). The spatial variation of $c(H\beta)$ follows the structure of the nebula, a characteristic also observed in NGC 40 (Leal-Ferreira *et al.* 2011) and NGC 7009 (Walsh *et al.* 2016). The histogram helps us to show that the spatial variation of $c(H\beta)$ is significant. If we use the full width half-maximum (FWHM) to (conservatively) determine the range where the variation is significant, we conclude that $0.18 < c(H\beta) < 0.34$. However, the radial profiles reinforce that $c(H\beta)$ in the outer region of the source reaches values higher than 0.40 (which could be linked to a higher dust-to-gas ratio, see Walsh *et al.* (2016) for a detailed discussion).

Acknowledgments: This work was supported by CNPq, Conselho Nacional de Desenvolvimento Científico e Tecnológico - Brazil, process numbers 248503/2013-8 (MLL-F) and 157806/2015-4 (IA) and by NWO/Netherlands.

References

Aleman, I., Leal-Ferreira, M. L., *et al.* in prep., *A&A*
 De Robertis, M., Dufour, J., & Hunt, R. 1987, *J. R. Astron. Soc. Canada*, 81, 195
 Kingsburgh, R. & Barlow, M. 1994, *MNRAS*, 271, 257

- Leal-Ferreira, M. L., Gonçalves, D. R., Monteiro, H., & Richards, J. W. 2011, *MNRAS*, 411, 1395
- Monteiro, H., Gonçalves, D. R., Leal-Ferreira, M. L., & Corradi, R. L. M. 2013, *A&A*, 560, 102
- Shaw, R. A. & Dufour, R. J. 1995, *PASP*, 107, 896
- Walsh J., Monreal-Ibero A., Barlow M., Ueta T., Wesson R., & Zijlstra A. 2016 *A&A*, 588, 106